BIOCHEMISTRY
including biophysical chemistry & molecular biology

Article

pubs.acs.org/biochemistry

Zn^{2+}-Induced Rearrangement of the Disordered TPPP/p25 Affects Its Microtubule Assembly and GTPase Activity

Ágnes Zotter,[†,⊥] Judit Oláh,[†,⊥] Emma Hlavanda,[†] Andrea Bodor,[‡] András Perczel,[‡] Krisztián Szigeti,[§] Judit Fidy,[§,∥] and Judit Ovádi*[,†]

[†]Institute of Enzymology, Biological Research Center, Hungarian Academy of Sciences, H-1113 Budapest, Hungary

[‡]Laboratory of Structural Chemistry and Biology, Institute of Chemistry, Eötvös Loránd University, H-1117 Budapest, Hungary

[§]Department of Biophysics and Radiation Biology, Semmelweis University, and [∥]Research Group for Membrane Biology, Hungarian Academy of Sciences-Semmelweis University, H-1094 Budapest, Hungary

ABSTRACT: Tubulin polymerization promoting protein/p25 (TPPP/p25) modulates the dynamics and stability of the microtubule system and plays crucial role in the myelination of oligodendrocytes. Here we showed by CD, fluorescence, and NMR spectroscopies that Zn^{2+} is the first ligand that induces considerable rearrangement of the disordered TPPP/p25. Zinc finger motif (His_2Cys_2) (His^{61}-Cys^{83}) was identified within the flexible region of TPPP/p25 straddled by extended unstructured N- and C-terminal regions. The specific binding of the Zn^{2+} to TPPP/p25 induced the formation of molten globule but not that of a well-defined tertiary structure. The Zn^{2+}-induced partially folded structure accommodating the zinc binding motif is localized at the single Trp^{76}-containing region as demonstrated by fluorescence resonance energy transfer and quenching experiments. We showed that the Zn^{2+}-induced change in the TPPP/p25 structure modified its interaction with tubulin and GTP coupled with functional consequences: the TPPP/p25-promoted tubulin polymerization was increased while the TPPP/p25-catalyzed GTPase activity was decreased as detected by turbidimetry and by malachite green phosphate release/^{31}P NMR assays, respectively. The finding that the Zn^{2+} of the bivalent cations can uniquely influence physiological relavant interactions significantly contributes to our understanding of the role of Zn^{2+}-related TPPP/p25 processes in the differentiation/myelination of oligodendrocytes possessing a high-affinity Zn^{2+} uptake mechanism.

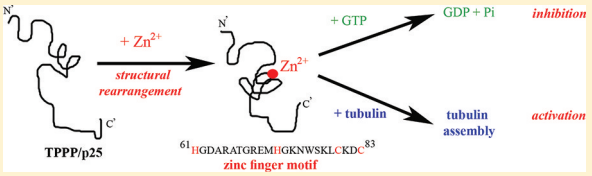

The proteins that do not have well-defined 3D structures or contain at least 30−40 amino acid long disordered segment(s), denoted as *intrinsically disordered* or *natively unfolded* proteins, are rather common in living cells and fulfill essential functions.[1−3] These proteins play crucial role in the etiology of neurological disorders such as Parkinson's and Alzheimer's diseases.[4,5] Tubulin polymerization promoting protein/p25 (TPPP/p25) is a disordered protein as judged by biophysical and biochemical data as well as predictions.[6,7] TPPP/p25 was isolated and identified as a brain-specific protein,[8] the primary target of which is the microtubule system, and it was denoted on the basis of its *in vitro* and *in vivo* function.[9,10] At physiological circumstances it is expressed predominantly in oligodendrocytes and plays role in the control of the dynamics and stability of the microtubule system as a microtubule-associated protein.[11] We have also postulated that, in addition to the bundling activity of TPPP/p25, it promotes the specific acetylation of α-tubulin on residue Lys^{40} affecting the dynamics of the microtubule system and microtubule-derived cell motility.[12] The specific expression of TPPP/p25 is crucial for the differentiation of oligodendrocytes likely via its role in the rearrangement of the microtubule network during the projection elongation prior to the onset of myelination.[13] The intracellular TPPP/p25 concentration was found to be controlled by the proteasome machinery at protein level as well as by specific microRNA at post-transcriptional level.[13,14] The moonlighting function of TPPP/p25 has recently been reported related to its pathological function.[15]

We identified two human gene sequences with 60% identity with that of the TPPP/p25 which encoded homologous proteins, TPPP2/p18 and TPPP3/p20.[16] These are shorter forms with missing N-terminal segment of TPPP/p25.[16] They could be clustered into three subfamilies present in mammals and other vertebrates.[17] While TPPP3/p20, similarly to TPPP/p25, specifically associates to the microtubule network with extensive bundling activity, TPPP2/p18 was found to be featured in much more ordered fashion; it did not bind to microtubules, but it distributed homogeneously within the cytosol of the transfected HeLa cells.[16] These data indicate that the two shorter homologues display distinct structural features that determine their microtubule-related functions *in vitro* as well as *in vivo*.[16]

Recently, we have shown that TPPP/p25 binds GTP and catalyzes its hydrolysis in a Mg^{2+}-dependent manner,[18] although no significant folding was detected in the presence of GTP by multinuclear NMR spectroscopy.[18] Multinuclear NMR analysis showed that extended unstructured segments of TPPP/p25 at the N- and C-terminals are localized straddling a

Received: July 20, 2011
Revised: October 13, 2011
Published: October 13, 2011

flexible region (130 aa). Such analysis was also performed with TPPP3/p20. Accordingly, it also has an unstructured C-terminal segment; however, a folded "core" involving α-helix structures was successfully assigned.[19] The main interacting partner of TPPP/p25 is tubulin, the binding of which to TPPP/p25 caused significant alteration in the CD spectrum attributed to the folding of the disordered TPPP/p25.[9] The folding potency of TPPP/p25 was proved when its CD spectrum was measured in the presence of trifluoroethanol, which resulted in an increase in the α-helix content from 4% to about 40%.[7]

In this work we identified a ligand, Zn^{2+}, a specific bivalent cation which bound to a well-characterized segment of the middle flexible region of TPPP/p25 resulting in alteration in the secondary but not in the tertiary structure. This structural change of the disordered TPPP/p25 was found to influence the TPPP/p25-promoted tubulin polymerization and GTPase activity.

EXPERIMENTAL PROCEDURES

Materials. Solutions were prepared with double-distilled, deionized water. Protein concentrations were measured by the Bradford method[20] using the Bio-Rad protein assay kit. GTP was obtained from Sigma-Aldrich (St. Louis, MO). GTP concentration was determined by UV−vis absorption spectroscopy by using an extinction coefficient of ε_{253} = 13 700 M^{-1} cm^{-1}. 1-Anilinonaphthalene-8-sulfonic acid (ANS) was obtained from Sigma-Aldrich (St. Louis, MO). Metal ions were always freshly dissolved in water.

Human Recombinant TPPP Proteins. Human recombinant TPPP proteins were expressed in *E. coli* BL21 (DE3) cells and isolated as described previously.[6,16]

Tubulin Preparation. Tubulin was purified from bovine brain by the method of Na and Timasheff.[21]

Isothermal Titration Calorimetry (ITC) Studies. ITC measurements were carried out with TPPP/p25 at 25 °C through direct titration mode (metal ion in the syringe) on a VP-ITC instrument (MicroCal, Piscataway, NJ). Typical titration experiments were performed by adding 2 mM Zn^{2+} or Ca^{2+} aliquots into the ITC cell containing 15 μM TPPP/p25 in 40 mM Tris buffer, pH 7.6, to obtain a final molar ratio of 1:14 for protein:metal ion. The titration data were corrected for small heat changes observed in background titration of the metal ion in the absence of the protein. The calorimetric data were analyzed by the Origin software provided by MicroCal.

CD Spectroscopy. CD measurements were performed on Jasco J-720 spectropolarimeter (Tokyo, Japan). Typical instrument conditions were as follows: scan rate 20 nm/min, time constant 8 s, step size 0.5 nm. Path length was 0.1 cm for far-UV studies and 1 cm for the near-UV region. In the far-UV experiments the protein concentrations were as follows: 4 μM for TPPPs and 1 μM for tubulin. Concentration was 20 μM for TPPP/p25 in the near-UV studies. Zinc ion concentration was varied from 50 to 200 μM. Measurements were carried out in 10 mM phosphate buffer, pH 7.0, at room temperature. The reaction mixtures were incubated for 10 min before recording the spectra. Scanning was repeated three times, and the spectra were averaged. Mean molar ellipticity (Θ) per residue in degrees square centimeter per decimole was calculated according to the following equation: $\Theta = \Theta_m/(10ncl)$, where θ_m is the measured ellipticity in millidegrees, n is the number of amino acid residues, c is the concentration in mol/L, and l is the path length of the cell in centimeters.

Fluorescence Spectroscopy. All fluorescence measurements were performed in 10 mM phosphate buffer, pH 7.0, using a Jobin Yvon Fluoromax-3 spectrofluorometer (Jobin Yvon Horiba, Longiumeau, France) at 25 °C. A quartz cuvette of 1 cm optical path length was used for each measurement. All measurements were done in triplicate. Data were processed using DataMax software.

ANS Binding. Freshly prepared 10 mM ANS stock solution made with distilled water was used for each experiment. The fluorophore was excited at 380 nm, and emission was monitored from 400 to 600 nm. The slits were adjusted to 2 nm. The ANS concentration was 50 μM, and the protein concentration was kept at 5 μM. A blank spectrum without protein was recorded before addition of the TPPP/p25 or its homologues.

Intrinsic Trp Fluorescence. The tryptophan fluorescence of 8 μM TPPP/p25 was examined at room temperature, in the absence and presence of increasing Zn^{2+} concentrations, from 0.5 to 40 μM. The excitation wavelength was maintained at 290 nm (10 nm slit width) while monitoring emission from 300 to 450 nm (2 nm slit width). The fluorescence resonance energy transfer (FRET) from Trp to ANS was also measured when Trp was excited at 290 nm in the absence and presence of 50 μM ANS. FRET experiments were performed at 2 μM final protein concentration. Emission spectra were recorded between 300 and 560 nm.

NMR Spectroscopy. *Multinuclear NMR Measurement.* Zn^{2+} binding studies were carried out using uniformly labeled 440 μM ^{15}N human recombinant TPPP/p25 sample which was prepared as described previously.[18] The [TPPP/p25]/[Zn^{2+}] ratio was 1:1 and 1:2. Measurements were performed in 50 mM Tris buffer, pH 6.8, at 300 K using a home-built 750 MHz NMR spectrometer, controlled with GE/Omega software and equipped with an Oxford Instruments Co. magnet and a home-built triple-resonance pulsed-field-gradient probe-head. All spectra were processed using the NMRPipe/nmrDraw software and with the public domain graphics program Sparky.

^{31}P NMR Measurements. 200 μM freshly prepared TPPP/p25 solution was typically used in 50 mM Tris buffer, at pH 6.8, containing 3 mM $MgCl_2$ and 1.0 mM GTP. The Zn^{2+} concentration was 400 μM. NMR measurements were performed at 298 K. GTPase activity was followed by ^{31}P NMR measurements at 101.25 MHz, on a Bruker Avance 250 MHz instrument, equipped with a 5 mm $^{13}C/^{19}F/^{31}P$ probe-head. 1D inverse gated ^{1}H decoupled spectra were collected using a 50 ppm spectral window, the number of scans varied between 3000 and 6000, and a 30° pulse and a relaxation delay of 2 s were applied. The course of GTP hydrolysis was recorded *in situ* by NMR. Spectra analysis was done using the TopSpin program.

ELISA. The plate was coated with 5 μg/mL (100 μL/well) tubulin solution in PBS overnight at 4 °C. The wells were blocked with 1 mg/mL BSA in PBS for 1 h at room temperature. Next, the plate was incubated with serial dilutions of TPPP/p25 for 1 h at room temperature in PBS. Where indicated, 100 μM Zn^{2+} without or with 500 μM EDTA was also present. Then the plate was sequentially incubated with the antibody produced against TPPP/p25 (1:5000),[6] and with the secondary IgG-peroxidase conjugate (1:5000, Sigma). Both antibodies were in PBS buffer containing 1 mg/mL BSA and incubated for 1 h at room temperature. Between each incubation step the wells were washed three times with PBS containing 0.05% Tween 20 for 10 min. The binding of the

antibody to the complexed TPPP/p25 was detected using *o*-phenylenediamine in the concentration of 3.7 mM with 0.03% peroxide as substrate solution. The peroxidase-catalyzed reaction was stopped after 10 min with 1 M H_2SO_4; absorbance was read at 490 nm by using a precision microplate reader (Wallac 1420, Perkin-Elmer).

Tubulin Polymerization Assay. The assembly of 8 μM tubulin was assessed in polymerization buffer (50 mM Mes, pH 6.6, containing 100 mM KCl, 1 mM dithioerythritol, 1 mM $MgCl_2$, and 1 mM EGTA) at 37 °C in the absence and presence of 100 μM Zn^{2+} or Ca^{2+}. The tubulin polymerization into microtubules was induced by the addition of 1.75 μM TPPP/p25 or 6 μM TPPP3/p20. The assembly of 10 μM tubulin was also assessed at 37 °C in the absence and presence of 100 μM Zn^{2+} induced by 20 μM paclitaxel. Optical density was monitored at 350 nm using a thermostated Cary 100 spectrophotometer (Varian, Walnut Creek, Australia).

Malachite Green Phosphate Release Assay. Malachite green phosphate release assay was performed as described previously.[18] The reaction mixture containing 80 μM freshly prepared TPPP/p25 was incubated at room temperature with 1500 μM GTP in the absence and presence of 150 μM Zn^{2+} in 20 mM Tris buffer, pH 7.4, containing 5 mM $MgCl_2$. The absorbance was measured at 660 nm by using a microplate reader (Wallac 1420, Perkin-Elmer). Control measurements were carried out with TPPP/p25 or nucleotide solutions alone. The control MgGTP hydrolysis was subtracted from that measured in the mixture of TPPP/p25 and MgGTP. The P_i calibration curve was determined with KH_2PO_4.

RESULTS

Zinc Binding Motif of the TPPP/p25. The sequences of TPPP proteins were analyzed for well-established ligand binding motifs which could be potential target for ligand-induced structural changes. Previously, we showed that TPPP/p25 has GTP-binding consensus motifs, and it binds, indeed, this nucleotide; however, the binding did not result in significant folding of this disordered protein.[18] Now we have identified a characteristic zinc binding motif, $His^{61}(Xaa)_{10}His^{72}(Xaa)_7Cys^{80}(Xaa)_2Cys^{83}$, within the middle, flexible region of TPPP/p25 (130 aa) (Figure 1). The two

Figure 1. Motifs of TPPP/p25 involved in ligand binding. The GTP-binding consensus P-loop motif ($G^{68}REMHGK^{74}$), the predicted zinc finger motif (61−83), and the tubulin binding domain (163−188) are indicated. The zinc binding motifs of the homologues proteins are indicated as well.

homologues of TPPP/p25 have only partial zinc finger motifs (Cys_2 for TPPP2/p18 and His_1Cys_2 for TPPP3/p20). Consequently, we expected that the zinc ion bound to TPPP homologues, if at all, with distinct characteristics. The zinc binding to the TPPP/p25 and the structural consequences were analyzed by biophysical and biochemical approaches; in some cases to test the specificity comparative studies were carried out with its homologous proteins and other metal ions as well.

Thermodynamic Characteristics of Zinc Binding. *Isothermal Titration Calorimetry.* ITC was performed by monitoring the heat changes that accompany metal ion binding to the TPPP/p25 in order to evaluate the thermodynamic parameters of the interaction. Calorimetric titrations with Zn^{2+} were carried out by adding aliquots of the bivalent cation to 40 mM Tris buffer, pH 7.6 with and without 15 μM TPPP/p25. The incremental additions of Zn^{2+} to TPPP/p25 were accompanied by significant heat change as compared to the control, indicating that the cation binds to the protein, while under similar conditions Ca^{2+} caused negligible heat effect even in the presence of TPPP/p25; therefore, no detectable Ca^{2+} binding was observed. As shown in Figure 2, the integrated heat

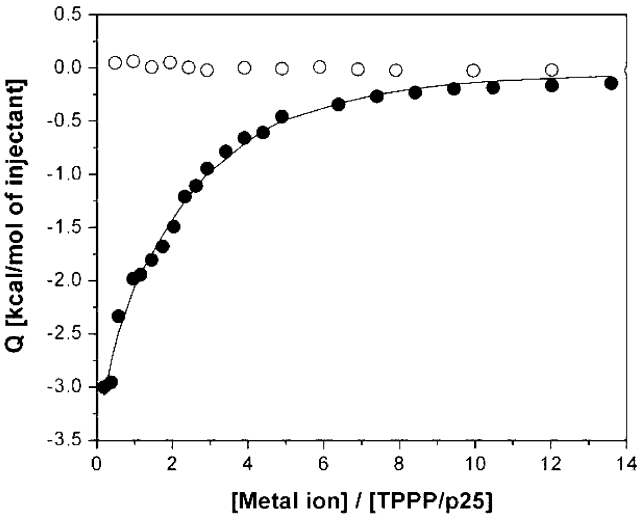

Figure 2. Representative calorimetric titrations of TPPP/p25 with Zn^{2+} and Ca^{2+}. The metal ions (syringe: 2 mM) were added to the protein solutions (calorimetric cell: 15 μM) at 25 °C in Tris buffer (pH 7.6). Titrations with Zn^{2+} (●) and with Ca^{2+} (○). The solid line represents the best fit of the Zn^{2+}-TPPP/p25 data to a model with one set of binding sites; the resulting fit parameters are $K_a = (3.29 \pm 0.64) \times 10^4$ M^{-1}; $n = 1.04 \pm 0.29$; $\Delta H = -9.42 \pm 3.06$ kcal mol^{-1}; $\Delta S = -10.9$ cal mol^{-1} K^{-1}. Three independent experiments were performed.

data of the Zn^{2+} titration could be fitted by the simplest binding model, which entails a single binding event (1 equiv of Zn^{2+} bound to the protein, $n = 1.04 \pm 0.29$) characterized by an association constant, $K_a = (3.29 \pm 0.64) \times 10^4$ M^{-1}. The ITC data indicated that Zn^{2+} binding to TPPP/p25 is an exothermic reaction with enthalpy change as deduced from the fitting data: ($\Delta H = -9.42 \pm 3.06$ kcal mol^{-1}, $T\Delta S = -3.25$ kcal mol^{-1}, $\Delta G = -6.17$ kcal mol^{-1}). The result from this study showed that the zinc ion is a potential interacting partner of TPPP/p25. The nature of this interaction is further analyzed at molecular level by various additional methods.

Zinc-Induced Structural Changes of TPPPs. The CD spectra of the TPPP/p25 in the far-UV and near-UV ranges were analyzed to obtain information about the effect of the Zn^{2+} binding on the secondary and tertiary structures, respectively. As shown in Figure 3A, TPPP/p25 displays spectral features characteristic for disordered proteins;[16,22,23] however, the addition of Zn^{2+} produced spectral change with two nearly identical minimum at 208 and 222 nm and a maximum around 190 nm, typical for α/β structure. This alteration is consistent with the observation that Zn^{2+} induces secondary structural changes of TPPP/p25 at the expense of

dx.doi.org/10.1021/bi201447w | *Biochemistry* 2011, 50, 9568−9578

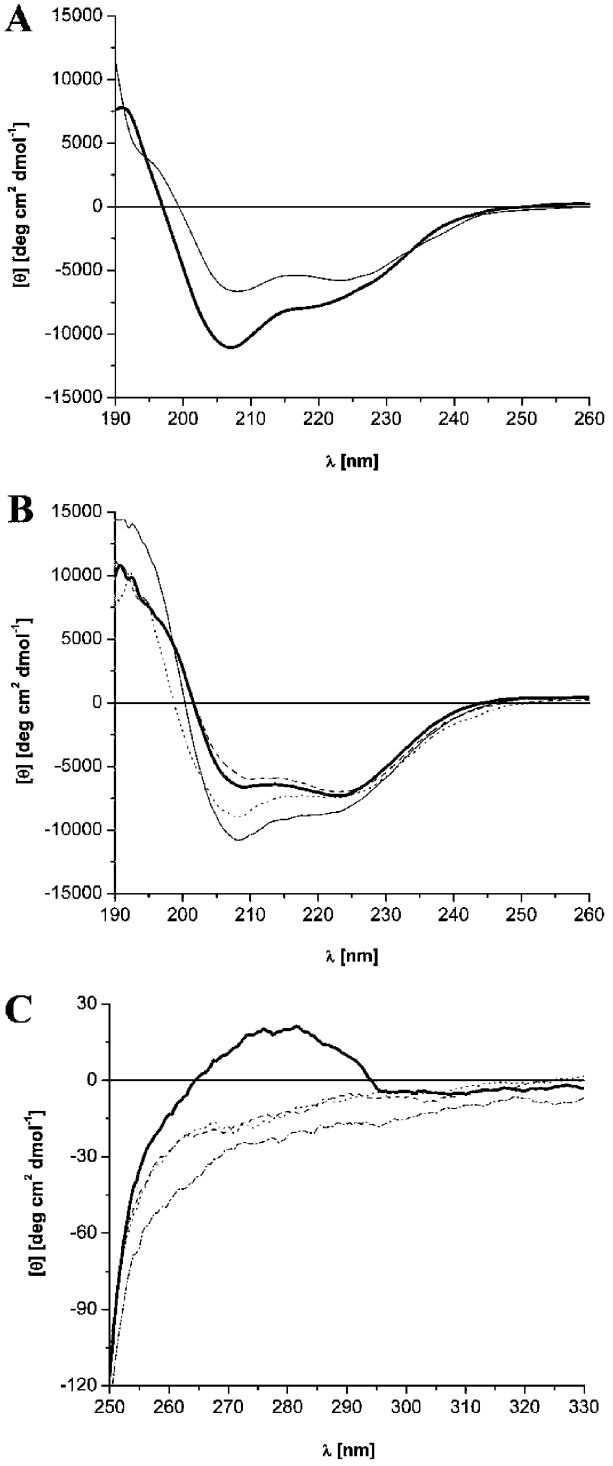

Figure 3. Effect of Zn^{2+} on the normalized far- and near-UV CD spectra of TPPP proteins. (A) Far-UV CD spectrum of TPPP/p25 (bold line) incubated with 200 μM Zn^{2+} ion (solid line). (B) CD spectrum of TPPP/p18 (bold line) incubated with 200 μM Zn^{2+} ion (dashed line) and that of TPPP/p20 (solid line) incubated with 200 μM Zn^{2+} ion (dotted line). (C) Near-UV CD spectra of TPPP/p25 in the absence and presence of Zn^{2+} ion. Concentrations of Zn^{2+} were as follows: none (bold line), 50 μM Zn^{2+} (dashed line), 100 μM Zn^{2+} (dotted line), and 200 μM Zn^{2+} (dash-dotted line). Three-five independent experiments were performed; error of determinations (SEM) for CD is ±5%.

the random coil structure. Other cations, such as Ni^{2+}, Al^{3+}, or Mg^{2+} ions used to study the specificity of zinc ion, did not alter the CD spectra (data not shown); therefore, the change in the secondary structure of the TPPP/p25 could be attributed exclusively to the binding of the Zn^{2+}.

A similar set of studies were performed with the two TPPP homologues, TPPP3/p20 and TPPP2/p18, which have His_1Cys_2 and Cys_2 residues, respectively, to test the specificity of the motif found in TPPP/p25 for zinc binding. The effects of Zn^{2+} on the far-UV CD spectra of the two homologues were recorded as well. As shown in Figure 3B, no significant alteration in the spectra of the two homologues was caused by the addition of Zn^{2+}, suggesting the necessity of a zinc finger motif found within the highly flexible region of TPPP/p25.

To obtain information whether the structural changes by Zn^{2+} is coupled with alteration in the tertiary structure of TPPP/p25, the near-UV CD spectra of the protein were recorded. As illustrated in Figure 3C, there was a measure of signal between the 270−290 nm region reflecting some tertiary structure, and this signal clearly disappeared by the addition of Zn^{2+}, indicating Zn^{2+}-induced structural rearrangement of TPPP/p25.

Zinc Induces Molten Globule Formation of TPPP/p25. To gain insight into the nature of the Zn^{2+}-induced structural changes of the TPPP/p25, in an additional set of experiments ANS fluorescence measurements were performed. ANS is frequently used to establish molten globule state since fluorescence of the hydrophobic ANS probe is much stronger in the presence of molten globular state than with a rigid, well-folded or fully unfolded state.[24,25] Thus, the increase in the fluorescence of ANS by its binding to proteins is one of the most efficient criteria for distinguishing between folded, molten globule, and unfolded states.[26] Figure 4A shows that, upon the addition of ANS to TPPP/p25, the fluorescence intensity increased displaying an emission spectrum with a maximum at 485 nm. By adding Zn^{2+}, the intensity further increased reaching saturation value at 20 μM Zn^{2+} concentration coupled with the blue shift (~12 nm) of the maximum of the emission spectrum. This effect seems to be specific for this bivalent cation since only a negligible increase and a slight blue shift in the TPPP/p25-ANS spectrum were detected with Ca^{2+} and Al^{3+}, as illustrated in Figure 4A. This means that in the presence of Zn^{2+} molten globule can be formed.

A similar sets of experiments were carried out with the homologous TPPP proteins. As illustrated in Figure 4B, the increase in the ANS fluorescence intensity was small, if at all, especially in the case of the folded TPPP2/p18. Thus, the Zn^{2+}, even if it binds to the homologous TPPPs, does not induce molten globule conformer(s) available for ANS binding even at 200 μM Zn^{2+} concentration. All these data suggest that a rather loosely packed hydrophobic core of TPPP/p25 likely exists within the middle, flexible region of TPPP/p25 where the zinc binding motif is localized, and the addition of Zn^{2+} promotes loose molten globule conformation with marginal stability, leading to structural rearrangement of the flexible region. This phenomenon was observed in the case of TPPP/p25 but not in the cases of its homologues. Although molten globule state can be induced in many proteins under extreme conditions, this is one of the few reported cases of such a structure under near physiological conditions.

Tryptophan Involved in the Molten Globule Conformer. TPPP/p25 has a single Trp (Trp^{76}) which is localized within the zinc finger motif as illustrated in Figure 1. We

dx.doi.org/10.1021/bi201447w | Biochemistry 2011, 50, 9568−9578

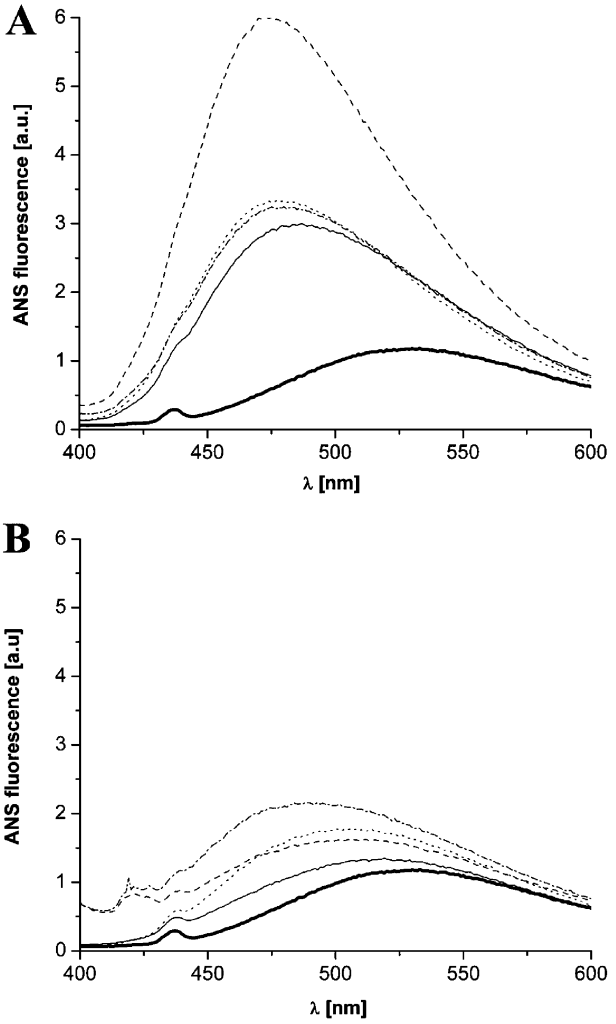

Figure 4. Effect of Zn^{2+} on the ANS fluorescence spectra of TPPP proteins. (A) Emission spectra of free ANS (bold line), ANS with TPPP/p25 (solid line), and ANS−TPPP/p25 with 20 μM Zn^{2+} (dashed line), ANS−TPPP/p25 with 20 μM Ca^{2+} (dotted line), and ANS−TPPP/p25 with 20 μM Al^{3+} (dash-dotted line). (B) Emission spectra of ANS (bold line) incubated with TPPP/p18 (solid line) or TPPP/p20 (dotted line), ANS-TPPP/p18 in the presence of 200 μM Zn^{2+} (dashed line), and ANS-TPPP/p20 with 200 μM Zn^{2+} (dash-dotted line). Measurements were carried out at 25 °C. Protein concentration was kept at 5 μM. ANS concentration was 50 μM. The displayed Zn^{2+} concentrations correspond to those where maximal effect was observed for each homologue. The fluorescence intensity is in arbitrary unit (a.u.). Three to five independent experiments were performed. Representative spectra are shown; error of determinations (SEM) for ANS fluorescence is ±10%.

showed that the binding of Zn^{2+} increased the ANS fluorescence intensity suggestive for the role of this bivalent cation in the formation of molten globule conformer. Fluorescence quenching and FRET experiments were performed to confirm the structural interrelation of the zinc binding motif, the single Trp residue, and the molten globule conformer judged by ANS.

In the first set of experiments, the Zn^{2+} effect on the intrinsic Trp fluorescence was analyzed. As shown in Figure 5A, the Trp emission with excitation at 290 nm was quenched by addition of Zn^{2+}, reaching the maximum effect at 40 μM cation concentration. Since we found that the addition of Zn^{2+} caused no significant quenching in the emission spectrum of Trp in a model compound (*N*-acetyltryptophanamide), it can be concluded that quenching effect was not due to its association to the single tryptophan (Trp^{76}) of TPPP/p25; the Zn^{2+} binding affects the neighborhood of the Trp^{76} of the protein. Figure 5B shows the dose-dependent effect of the Zn^{2+} on the intensity and the maximum position of the Trp emission spectrum of TPPP/p25. The increase of Zn^{2+} concentration resulted in a substantial decrease in fluorescence intensity coupled with a pronounced red shift (~19 nm) of the Trp λ_{max}. Ca^{2+}, another bivalent cation, displayed much less effect on the fluorescence characteristics of Trp of TPPP/p25 as shown in Figure 5C. These observations indicate that Ca^{2+} does not affect significantly the intrinsic fluorescence of TPPP/p25 and corroborate the specificity of Zn^{2+} binding to this protein, in agreement with the ITC results.

In the second set of experiments FRET measurements with ANS provided evidence for the neighborhood of Trp and TPPP/p25-bound ANS characteristic for molten globule state. Excitation of the protein at 290 nm resulted in a Trp emission band at ~340 nm, whereas ANS solution excited at the same wavelength has only background emission. As shown in Figure 5D, the emission of Trp excited at 290 nm was reduced in the presence of ANS, while the ANS emission increased. This finding shows that the energy transfer occurred in this system, confirming that the Trp^{76} (donor) and the TPPP/p25-bound ANS (acceptor) are in the vicinity of each other in the flexible region of TPPP/p25 at the potential zinc binding site.

Effect of Zinc Ion on the HSQC Spectrum of TPPP/p25. A powerful approach to follow the Zn^{2+} binding to TPPP/p25 is the two-dimensional NMR spectroscopy using ^{15}N-labeled protein. In a recent paper we have reported the assignment of the extended disordered segments of TPPP/p25 localized at the N- and C-terminals, while the flexible middle region could not be assigned.[18] As Zn^{2+} is a spectroscopically silent cation, its coordination can be followed by monitoring the variation of TPPP/p25 peaks in the HSQC spectra. Successive addition of Zn^{2+} to a 440 μM ^{15}N-labeled TPPP/p25 sample caused unambiguous variation in the intensity of several peaks, and these major spectral changes could be detected below 880 μM Zn^{2+} concentration.

As illustrated in Figure 6A, as a consequence of successive Zn^{2+} addition most of the peaks in the corresponding HSQC spectrum disappeared. Since TPPP/p25 is abundant in glycine residues spreading over the unstructured (assigned) terminals as well as the middle, flexible (unassigned) region, moreover, the Gly region is well-separated in the HSQC spectrum; thus, their analysis rendered it possible to suggest a region of TPPP/p25 affected by the zinc binding. Accordingly, four Gly residues of the N terminus (Gly^{20}, Gly^{37}, Gly^{39}, Gly^{41}) and eight of the nine residues of the C terminus (Gly^{184}, Gly^{186}, Gly^{188}, Gly^{191} Gly^{200}, Gly^{209}, Gly^{217}, Gly^{218}) were assigned as demonstrated in Figure 6B. The additional Gly residues localized mainly in the middle flexible region of the TPPP/p25 showed low intensity or are broadened to the baseline preventing the assignation. We found that the intensities of the assigned Gly residues at equimolar concentration of TPPP/p25 and Zn^{2+} were maintained although in the case of three ones localized in the C-terminus (Gly^{209}, Gly^{217}, Gly^{218}) the intensity was slightly decreased. At double Zn^{2+} concentration slight reduction of the intensities of Gly^{41}, Gly^{186}, and Gly^{188} was observed. These data suggest that a unique Zn^{2+} could be coordinated within the unassigned core region of TPPP/p25 causing structural change.

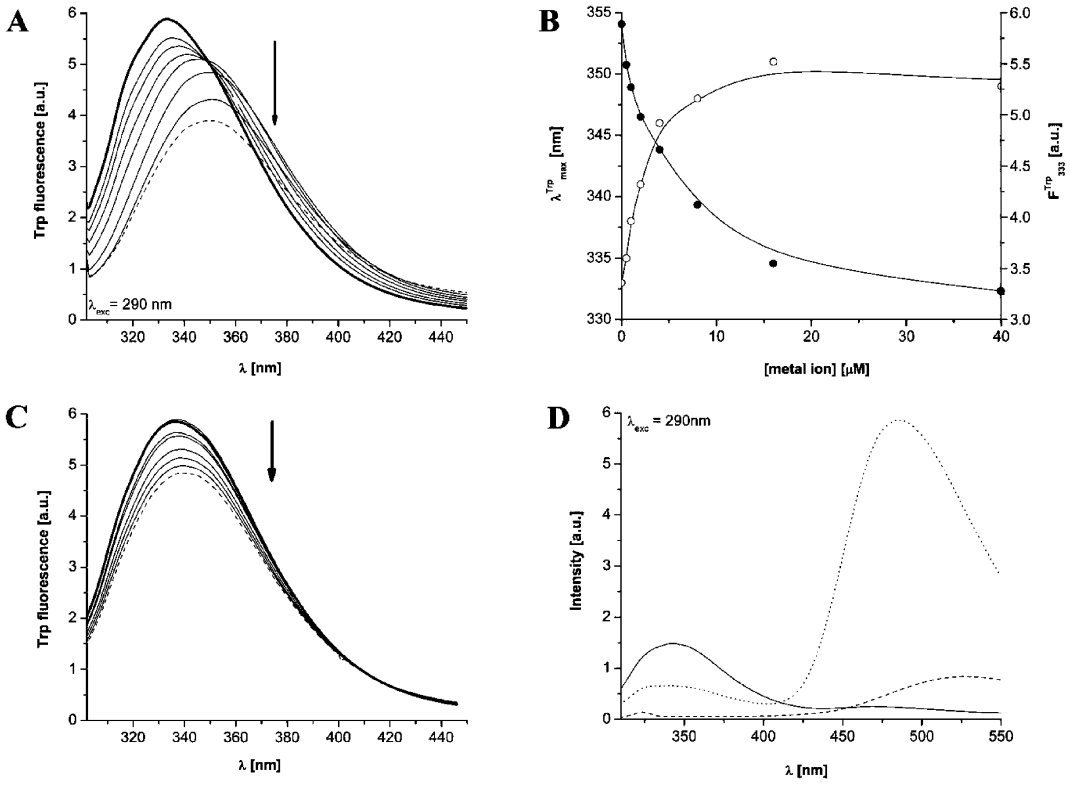

Figure 5. Effect of metal ions on the Trp fluorescence spectrum of TPPP/p25. (A) Intrinsic Trp fluorescence spectra measured for 8 μM TPPP/p25 (bold line), TPPP/p25 in the presence of increasing Zn^{2+} concentrations (40 μM: dashed line) in independent experiments (arrow indicates the increase in Zn^{2+}concentrations: 0.5, 1, 2, 4, 8, 16, and 40 μM, respectively). (B) Effect of zinc ions on TPPP/p25 intrinsic fluorescence: position of the tryptophan fluorescence spectrum maximum (open symbols), fluorescence intensity at λ_{333} (black symbols). Protein concentration was kept at 8 μM. (C) Effect of calcium ions on TPPP/p25 intrinsic fluorescence. 8 μM TPPP/p25 (bold line), TPPP/p25 in the presence of increasing Ca^{2+} concentrations (40 μM: dashed line) in independent experiments (arrow indicates the increase in Ca^{2+}concentrations: 0.5, 1, 2, 4, 8, 16, and 40 μM). (D) Fluorescence resonance energy transfer between Trp and ANS. Fluorescence emission spectra obtained upon excitation at 290 nm of TPPP/p25 (solid line), of free ANS in solution (dashed line), and of the TPPP/p25-ANS complex (dotted line). The fluorescence intensity is in arbitrary unit (a.u.). Three to five independent experiments were performed. Representative spectra are shown; error of determinations (SEM) for Trp fluorescence is ±10%.

Effect of Zinc on TPPP/p25–Tubulin Interaction. Previously, we showed that the major target of TPPP/p25 is the tubulin/microtubule system both *in vitro* and *in vivo*.[9,10] The interaction of TPPP/p25 with tubulin induces structural change as indicated by the difference ellipticity spectrum in the far-UV range detected by CD spectroscopy that is likely originated from the change in the structure of the disordered TPPP/p25.[9] Our present data show that the addition of Zn^{2+} to the TPPP/p25–tubulin complex modifies this spectral change in the 200–230 nm region, suggesting changes for α/β structure as shown in Figure 7A. Therefore, this finding reveals that the Zn^{2+}-induced structural alteration manifests itself in the structure of TPPP/p25–tubulin complex. It is important to emphasis that the Zn^{2+} does not tend to disrupt the TPPP/p25–tubulin complex or prevent their association as noticed even at high excess of the cation concentration as supported by ELISA experiments as well. Figure 7B shows that the binding of TPPP/p25 to the immobilized tubulin detected by specific TPPP/p25 antibody occurred at similar TPPP/p25 concentration in the presence of Zn^{2+}, although the saturation level was slightly lower. This phenomenon could be attributed to the hindered formation of the immunocomplex due to the Zn^{2+}-induced structural alteration of the TPPP/p25–tubulin complex resulting in reduced epitope availability for the TPPP/p25 antibody.

A basic function of TPPP/p25 is its tubulin polymerization promoting activity which can be assayed by *in vitro* turbidity measurement as described previously.[9] Figure 7C reveals that TPPP/p25 promotes the tubulin polymerization as detected by the enhancement of the turbidity, a rapid increase in the absorbance at 350 nm reaching a quasi-equilibrium state. This assay was used to monitor the effect of Zn^{2+} binding to the TPPP/p25 on its tubulin polymerization promoting activity. The polymerization process was enhanced by Zn^{2+}, but not by the Ca^{2+}, as compared to the control which is indicative, in agreement with the binding data, for this cation-induced structural alteration in the TPPP/p25–tubulin complex.

In order to test whether this effect is due to the binding of Zn^{2+} directly to the microtubule or the effect of zinc ion manifested itself via its association to TPPP/p25, control experiments were performed by measuring the Zn^{2+} effect on the tubulin polymerization in the absence of TPPP/p25. Accordingly, the tubulin assembly was induced by paclitaxel or TPPP3/p20, a TPPP/p25 homologue protein which is able to induce tubulin polymerization but it does not have zinc finger motif. As illustrated in Figure 7D, Zn^{2+} effect on the tubulin polymerization was not detected, suggesting that the alteration induced by Zn^{2+} on the tubulin polymerization appears to be specific for TPPP/p25 and it does not originate from the Zn^{2+} binding to the tubulin. The finding that the Zn^{2+}-bound TPPP/

dx.doi.org/10.1021/bi201447w | *Biochemistry* 2011, 50, 9568–9578

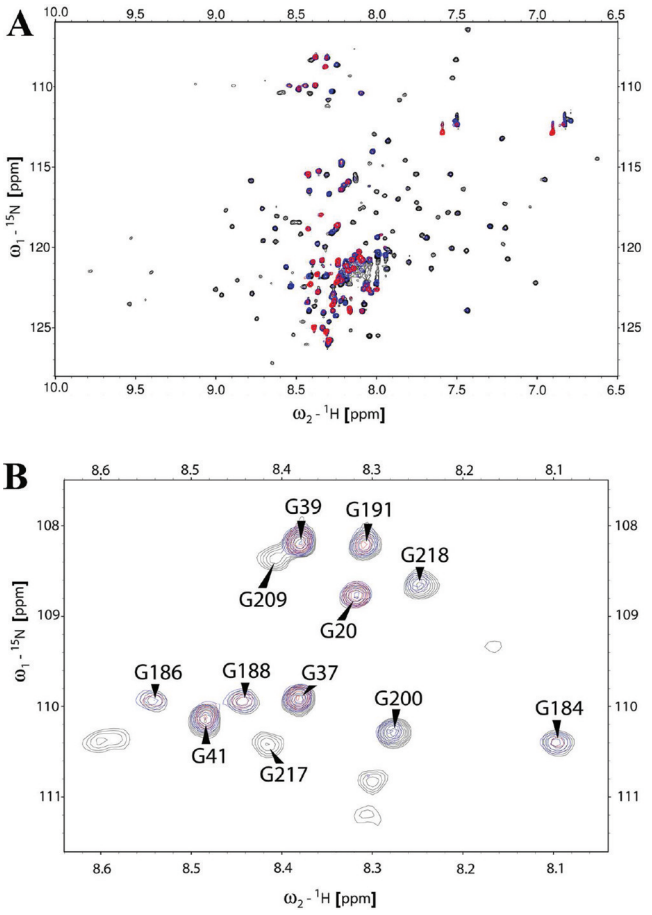

Figure 6. NMR characterization of Zn^{2+} binding. (A) Overlap of HSQC spectra recorded at 750 MHz of 440 μM ^{15}N-labeled TPPP/p25 (black) at 1:1 (blue) and 2:1 (red) Zn^{2+}:TPPP/p25 ratio. (B) The same spectra zoomed to the Gly region.

p25 is able to associate to tubulin is not surprising, since the tubulin binding domain of TPPP/p25 predicted on the basis of tau homology (163−188 aa)[23] does not overlap with the zinc finger motif (cf. Figure 1).

Effect of Zinc on TPPP/p25-Catalyzed GTP Hydrolysis. Recently, we have reported that GTP binds to TPPP/p25 which catalyzes the hydrolysis of this nucleotide.[18] We also showed by the malachite green phosphate release assay the crucial role of the Mg^{2+} in the TPPP/p25-derived GTP hydrolysis; no other bivalent cation including Zn^{2+} was able to replace Mg^{2+}. In this assay the concentration of the inorganic phosphate released by the hydrolysis of added GTP was detected as a function of time (Figure 8A). Since a potential GTP binding motif overlaps with the zinc finger motif within the middle flexible region of TPPP/p25 (cf. Figure1), the influence of this bivalent cation was tested on the GTPase activity of TPPP/p25. As shown in Figure 8A, the time-dependent formation of P_i from GTP in the presence of TPPP/p25 was partially inhibited by Zn^{2+} as detected by malachite green phosphate release assay. The maximum inhibition (around 50%) was reached at 150 μM Zn^{2+} concentration. Under these conditions GTPase activity of TPPP/p25 was reduced by 50% from k_{cat} = 0.018 min^{-1} to $k_{cat}^{Zn^{2+}}$ = 0.009 min^{-1}, while other bivalent cations, such as Fe^{2+} or Ca^{2+}, did not influence the GTPase activity of TPPP/p25 under similar conditions (data not shown).

Inhibition of GTPase activity by Zn^{2+} was also followed by ^{31}P NMR spectroscopy monitoring at the same time both the decrease of the characteristic GTP signals and the increase of the released inorganic phosphate (P_i) and other product formation, as described previously.[18] Figure 8 shows representative $^{31}P\{^1H\}$ spectra of TPPP/p25-catalyzed hydrolysis reaction in the absence (Figure 8C) and presence (Figure 8D) of 400 μM Zn^{2+} under similar conditions used in malachite green phosphate release assay. For NMR measurements a relatively high TPPP/p25 concentration (200 μM) was used in the presence of GTP, and Zn^{2+} addition resulted in a slightly turbid solution. This had no effect on the signal intensities in the one-dimensional spectra as compared to the solution without Zn^{2+}, but the presence of the metal ion caused significant line broadening on the peaks belonging to GTP, leaving the free P_i signal unaffected (Figure 8D). This phenomenon can be interpreted by chemical exchange reaction(s) on the NMR time scale due to Zn^{2+} binding involving the GTP phosphorus environment.[27,28] The time-dependent hydrolysis rate of GTP was evaluated from the integrated intensity of the released P_i signal (Figure 8B). The k_{cat} values of the GTPase activity of TPPP/p25 were k_{cat} = 0.0183 min^{-1} and $k_{cat}^{Zn^{2+}}$ = 0.0122 min^{-1} in the absence and presence of Zn^{2+}, respectively, which show good agreement with the rate constants obtained from the malachite green assay. The partial inhibition caused specifically by Zn^{2+} on the GTPase activity of TPPP/p25 suggests that the TPPP/p25−Zn^{2+} complex displays reduced potency which could be due to the competition of the Zn^{2+} and GTP for the binding and/or structural change on TPPP/p25.

DISCUSSION

A couple of biochemical and biophysical studies have suggested that TPPP/p25 does not have well-defined 3D structure; it is a disordered, intrinsically unstructured protein.[7,9−11] Recently, we have shown by multinuclear NMR that this protein has extended disordered segments at the N- and C-terminals straddling a highly flexible region.[18] In addition, we also reported that homologues TPPP proteins, TPPP3/p20 and TPPP2/p18, in spite of their high homology, display distinct structural and functional characteristics which cannot be attributed exclusively to the lack of the unstructured N-terminal region of TPPP/p25.[16] The structure of TPPP3/p20 (2JRF) determined by multinuclear NMR reveals the existence of an α-helix-containing core with a long disordered C-terminal region.[19] Although there is no direct data for the existence of such a core structure in the case of TPPP/p25, in the present work we were able to detect the formation of molten globule state enhanced by the Zn^{2+} binding. In fact, this is the first demonstration that a ligand can affect the disordered state of this protein.

We showed that Zn^{2+} induces structural rearrangement of TPPP/p25 suggesting that the specific binding of Zn^{2+} cation is coupled with conformational rearrangements probably leading to the stabilization of a not-defined segment of the middle flexible region of TPPP/p25. This segment includes a zinc finger motif, a GTP-binding motif, and the single Trp residue in the vicinity of a unique hydrophobic region targeted by ANS (cf. Figure 1).

The Zn^{2+} likely binds to the classical zinc finger motif, His_2Cys_2, identified by sequence alignment (cf. Figure 1). The existence of molten globule state was not demonstrated by

dx.doi.org/10.1021/bi201447w | Biochemistry 2011, 50, 9568−9578

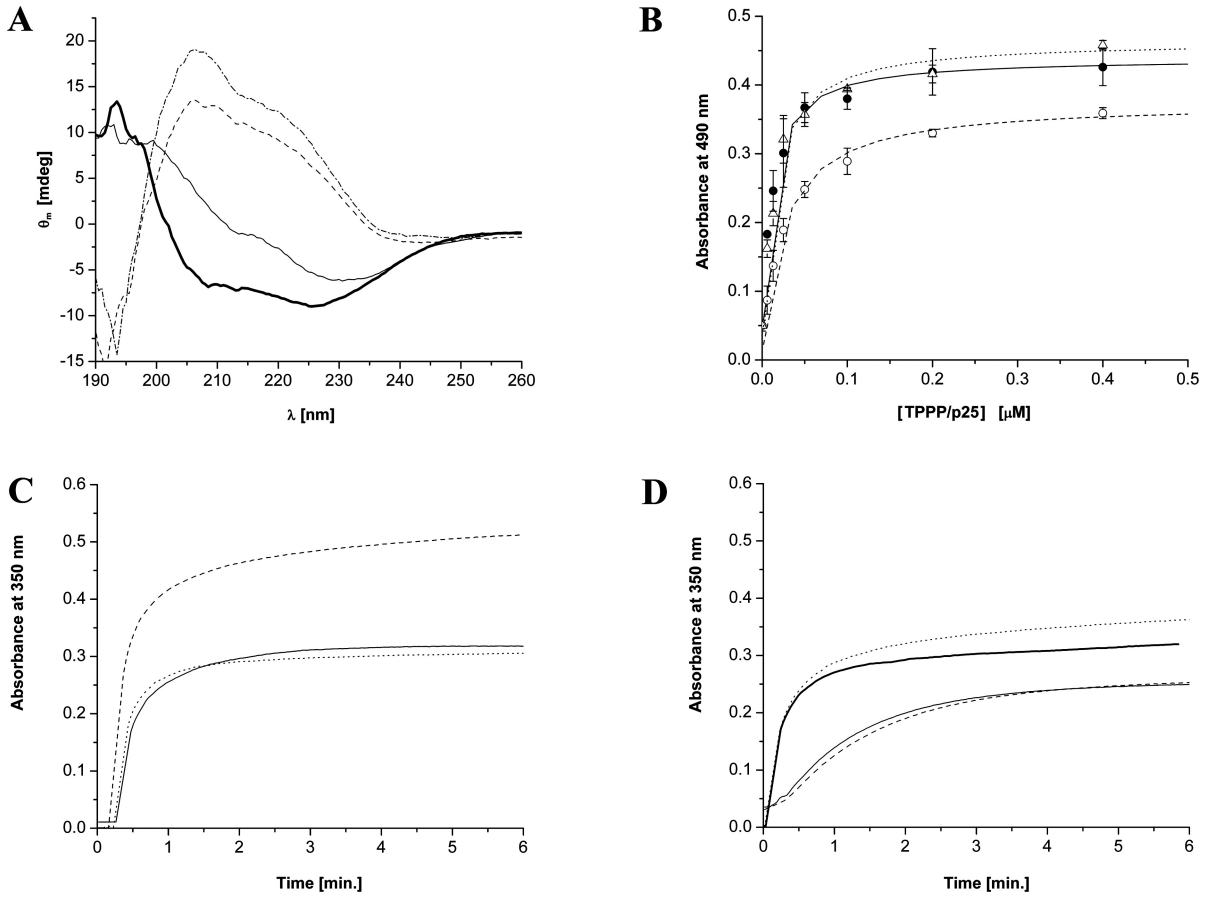

Figure 7. Effect of Zn^{2+} on the TPPP/p25–tubulin interaction. (A) Far-UV CD spectra of 4 μM TPPP/p25 and 1 μM tubulin complex (bold line) and that of terner complex containing 200 μM Zn^{2+} ion (solid line). Difference CD spectra for TPPP/p25–tubulin complex (dashed line) and for terner complex (dash-dotted line). Difference ellipticity was calculated by subtracting the ellipticities of TPPP/p25 and tubulin from that measured with the mixture of TPPP/p25 and tubulin or by subtracting the ellipticity of TPPP/p25–Zn^{2+} and tubulin–Zn^{2+} from that measured with the mixture of TPPP/p25, tubulin, and Zn^{2+}. (B) ELISA. The plate was coated with tubulin, then it was incubated with TPPP/p25 (●) at different concentrations in the presence of 100 μM Zn^{2+} (○) or 100 μM Zn^{2+} and 500 μM EDTA (△). The average of three independent experiments and the SEM are shown. (C) TPPP/p25-induced polymerization in the absence and presence of Zn^{2+}. 8 μM tubulin polymerization was induced by the addition of 1.75 μM TPPP/p25 (solid line) in the presence of 100 μM Zn^{2+} (dashed line) or 100 μM Ca^{2+} (dotted line) at 37 °C as described in the Experimental Procedures. Three independent experiments were performed. Representative polymerization is shown; error of determinations (SEM) is ±10%. (D) TPPP3/p20-induced polymerization in the absence (bold line) and presence of 100 μM Zn^{2+} (dotted line). Eight μM tubulin polymerization was induced by the addition of 6 μM TPPP3/p20. Paclitaxel-induced polymerization in the absence (solid line) and presence of 100 μM Zn^{2+} (dashed line). Three independent experiments were performed. Representative polymerization is shown; error of determinations (SEM) is ±10%.

ANS fluorescence spectroscopic measurement for the two homologues (cf. Figure 4) which can be attributed to structural differences of the TPPP proteins: the homologues possess folded structures and only a partial zinc finger motif. Consequently, the structural consequence observed at the Zn^{2+} binding to TPPP/p25 is unique for this protein; it was not observed with its homologues (cf. Figures 3 and 4); apparently, it requires a His_2Cys_2 binding motif situated in a highly flexible region.

In this work we showed that Zn^{2+} can influence the functional properties of TPPP/p25. We found that the Zn^{2+}-promoted structural rearrangement of TPPP/p25 enhanced the microtubule assembly (cf. Figure 7), while it inhibited the TPPP/p25-catalyzed GTP hydrolysis (cf. Figure 8). The influence of Zn^{2+} on the activity of this disordered protein at physiological conditions seems to be relevant being tubulin and microtubule system are its major target. Thus, the dynamics and stability of the microtubule system could be modified by the intracellular Zn^{2+} concentration which is relatively high in brain tissue (cf. see later). In contrast to the relationship of TPPP/p25 with the microtubule system, which is relatively well-established, there is limited amount of information concerning the significance of the TPPP/p25-catalyzed GTP hydrolysis.[18]

TPPP/p25 effectively catalyzes the GTP hydrolysis in a Mg^{2+}-dependent manner.[18] We revealed that TPPP/p25 binds GTP and suggested that a potential GTP-binding motif, the P-loop motif (G^{68}REMHGK^{74}), likely plays a significant role in its binding to TPPP/p25. This motif is localized within the flexible region of TPPP/p25 and overlaps with the zinc finger motif. It could be hypothesized in the light of these data that the inhibitory effect of Zn^{2+} on the TPPP/p25-catalyzed GTP hydrolysis is resulted from the competition of the two ligands for the overlapping binding motifs. It is equally possible that the two ligands compete not for the binding motifs rather for the conformation resulting in inhibition of the GTPase activity of the protein. It seems that the Zn^{2+}-induced partial folding is unfavorable for the highly flexible TPPP/p25 to adapt unique

dx.doi.org/10.1021/bi201447w | Biochemistry 2011, 50, 9568–9578

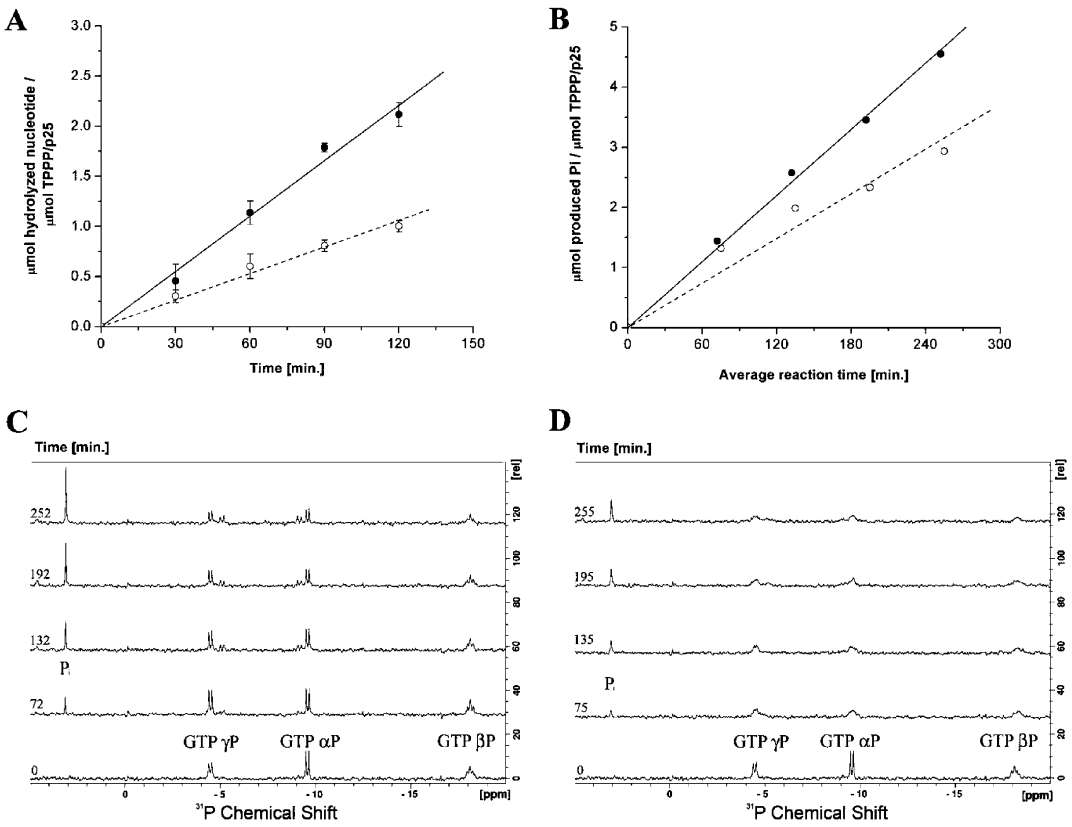

Figure 8. Zn^{2+} effect on the TPPP/p25-catalyzed GTP hydrolysis. (A) GTPase activity of TPPP/p25 measured by malachite green phosphate release assay in 20 mM Tris, pH 7.4 buffer containing 5 mM $MgCl_2$ in the absence (●) and presence (○) of 150 μM Zn^{2+}. GTP concentration was 1500 μM; protein concentration was 80 μM. k_{cat} values were determined by linear fitting of the initial rates (without Zn^{2+}: k_{cat} = 0.018 ± 0.001 min^{-1}, solid line; with Zn^{2+}: $k_{cat}^{Zn^{2+}}$ = 0.0088 ± 0.0009 min^{-1}, dashed line) using the Microcal Origin version 7.0 software (Microcal Software Inc.). The average of three independent sets of experiments and the SEM are shown. (B) Representative time course of the ^{31}P measurements in the absence (●) and presence (○) of 400 μM Zn^{2+}. The P_i concentration was determined from the integrated area of P_i peak. The release of P_i concentrations leads after linear fitting to k_{cat} = 0.0183 min^{-1} and $k_{cat}^{Zn^{2+}}$ = 0.0122 min^{-1}. Representative ^{31}P kinetic spectra of GTP hydrolysis and product formation catalyzed by TPPP/p25 in the absence (C) and presence (D) of 400 μM Zn^{2+}. Reaction of 200 μM TPPP/p25, 1 mM GTP, 3 mM Mg^{2+}, and 400 μM Zn^{2+} where is indicated in 50 mM Tris buffer at pH 6.8 is monitored by $^{31}P\{^1H\}$ NMR measurements at 101.25 MHz. Corresponding chemical shifts in ppm are GTP (α, β, γ): −9.52, −18.04, −4.40 and P_i: 3.08.

local conformation necessary for its GTPase activity. In a recent work we have suggested that TPPP/p25 might have functions similar to that of the small G proteins, which also display low endogenous GTPase activity.[18] In this paper we demonstrated by two independent methods that Zn^{2+} can modify the GTPase activity of the disordered TPPP/p25.

Zinc ion, the second most abundant trace element in the human body, is essential for the structural stability of a variety of proteins involved in transcription, protein trafficking, and enzyme catalytic activity.[29,30] The brain has the highest zinc concentration as compared to other organs; the average of total brain zinc concentration was estimated to be around 150 μM. The free zinc concentration is usually in the nanomolar range; however, the zinc content in the synaptic vesicles of some neurons was found to be more than 1 mM.[31] Oligodendrocyte progenitor cells accumulate Zn^{2+} via a high affinity and saturable Zn^{2+} transport mechanism which is sensitive to acidic pH and divalent metal ions. Several lines of evidence indicate that Zn^{2+} may modulate the activity of neurotransmitter receptors by possessing a potential neuromodulatory role.[32] In myelinating oligodendrocytes, where the myelin basic protein (MBP) and the TPPP/p25 are endogenously expressed and play a crucial role in the differentiation of the progenitor oligodendrocytes, the intracellular Zn^{2+} concentration is relatively high.[30]

The MBP is a disordered myelin protein similarly to TPPP/p25. It is one of the essential components for maintaining the stability of the myelin sheath of the CNS. Another stabilizing component of the myelin sheath is zinc, with a concentration about 50 μM.[33] Almost all of the zinc is in a protein-bound form, and MBP is a crucial zinc-binding protein with a dissociation constant in the low micromolar range (15−45 μM for the different forms of MBP). The binding of the zinc to the protein results in the stabilization of its association to myelin membranes and induces a compaction of the extended protein.[34] MBP is an effective interacting partner of TPPP/p25,[35] which might be essential for maintaining the integrity of the myelin sheath. Thus, it seems it could be hypothesized that Zn^{2+} is essential for mammalian brain physiology and may also play an important role in inducing neurodegeneration during acute CNS insults.[30]

AUTHOR INFORMATION

Corresponding Author

*Tel: (36-1) 279-3129. Fax: (36-1) 466-5465. E-mail: ovadi@enzim.hu.

Author Contributions

[⊥]These authors equally contributed to the work.

Funding

This work was supported by the Hungarian National Scientific Research Fund−OTKA [T-067963] to J. Ovádi, [PD-76793] to J. Oláh, [K84271] to J. Fidy, and [K72973] to A. Perczel; the European Commission [(DCI-ALA/19.09.01/10/21526/245-297/ALFA 111(2010)29] to J. Ovádi; European Concerted Research Action [COST Action TD0905] to J. Ovádi; János Bolyai Research Scholarship of the Hungarian Academy of Sciences to J. Oláh and A. Bodor; and Trans- National EC Research Infrastructure East-NMR (Contract No. 228461) at Oxford Facility. The European Union and the European Social Fund have provided financial support to the project under the grant agreement no. TÁMOP [4.2.1./B-09/KMR-2010-0003] to A. Perczel and A. Bodor.

■ ABBREVIATIONS

ANS, 1-anilinonaphthalene-8-sulfonic acid; FRET, fluorescence resonance energy transfer; ITC, isothermal titration calorimetry; MBP, myelin basic protein; TPPP/p25, tubulin polymerization promoting protein/p25.

■ REFERENCES

(1) Dunker, A. K., Brown, C. J., Lawson, J. D., Iakoucheva, L. M., and Obradovic, Z. (2002) Intrinsic disorder and protein function. *Biochemistry 41*, 6573−6582.

(2) Sickmeier, M., Hamilton, J. A., LeGall, T., Vacic, V., Cortese, M. S., Tantos, A., Szabó, B., Tompa, P., Chen, J., Uversky, V. N., Obradovic, Z., and Dunker, A. K. (2007) DisProt: the Database of Disordered Proteins. *Nucleic Acids Res. 35*, D786−793.

(3) Fink, A. L. (2005) Natively unfolded proteins. *Curr. Opin. Struct. Biol. 15*, 35−41.

(4) Uversky, V. N. (2002) What does it mean to be natively unfolded? *Eur. J. Biochem. 269*, 2−12.

(5) Ovádi, J., and Orosz, F. (2009) *Protein Folding and Misfolding: Neurodegenerative Diseases*, Springer, Berlin.

(6) Kovacs, G. G., László, L., Kovács, J., Jensen, P. H., Lindersson, E., Botond, G., Molnár, T., Perczel, A., Hudecz, F., Mező, G., Erdei, A., Tirián, L., Lehotzky, A., Gelpi, E., Budka, H., and Ovádi, J. (2004) Natively unfolded tubulin polymerization promoting protein TPPP/p25 is a common marker of alpha-synucleinopathies. *Neurobiol. Dis. 17*, 155−162.

(7) Orosz, F., Kovács, G. G., Lehotzky, A., Oláh, J., Vincze, O., and Ovádi, J. (2004) TPPP/p25: from unfolded protein to misfolding disease: prediction and experiments. *Biol. Cell 96*, 701−711.

(8) Takahashi, M., Tomizawa, K., Fujita, S. C., Sato, K., Uchida, T., and Imahori, K. (1993) A brain-specific protein p25 is localized and associated with oligodendrocytes, neuropil, and fiber-like structures of the CA hippocampal region in the rat brain. *J. Neurochem. 60*, 228−235.

(9) Hlavanda, E., Kovács, J., Oláh, J., Orosz, F., Medzihradszky, K. F., and Ovádi, J. (2002) Brain-specific p25 protein binds to tubulin and microtubules and induces aberrant microtubule assemblies at substoichiometric concentrations. *Biochemistry 41*, 8657−8664.

(10) Tirián, L., Hlavanda, E., Oláh, J., Horváth, I., Orosz, F., Szabó, B., Kovács, J., Szabad, J., and Ovádi, J. (2003) TPPP/p25 promotes tubulin assemblies and blocks mitotic spindle formation. *Proc. Natl. Acad. Sci. U. S. A. 100*, 13976−13981.

(11) Ovádi, J., and Orosz, F. (2009) An unstructured protein with destructive potential: TPPP/p25 in neurodegeneration. *Bioessays 31*, 676−686.

(12) Tőkési, N., Lehotzky, A., Horváth, I., Szabó, B., Oláh, J., Lau, P., and Ovádi, J. (2010) TPPP/p25 promotes tubulin acetylation by inhibiting histone deacetylase 6. *J. Biol. Chem. 285*, 17896−17906.

(13) Lehotzky, A., Lau, P., Tőkési, N., Muja, N., Hudson, L. D., and Ovádi, J. (2009) Tubulin polymerization-promoting protein (TPPP/p25) is critical for oligodendrocyte differentiation. *Glia 58*, 157−168.

(14) Lehotzky, A., Tirián, L., Tőkési, N., Lénárt, P., Szabó, B., Kovács, J., and Ovádi, J. (2004) Dynamic targeting of microtubules by TPPP/p25 affects cell survival. *J. Cell. Sci. 117*, 6249−6259.

(15) Ovádi, J. (2011) Moonlighting proteins in neurological disorders. *IUBMB Life 63*, 453−456.

(16) Vincze, O., Tőkési, N., Oláh, J., Hlavanda, E., Zotter, Á., Horváth, I., Lehotzky, A., Tirián, L., Medzihradszky, K. F., Kovács, J., Orosz, F., and Ovádi, J. (2006) Tubulin polymerization promoting proteins (TPPPs): members of a new family with distinct structures and functions. *Biochemistry 45*, 13818−13826.

(17) Orosz, F., and Ovádi, J. (2008) TPPP orthologs are ciliary proteins. *FEBS Lett. 582*, 3757−3764.

(18) Zotter, Á., Bodor, A., Oláh, J., Hlavanda, E., Orosz, F., Perczel, A., and Ovádi, J. (2011) Disordered TPPP/p25 binds GTP and displays Mg(2+)-dependent GTPase activity. *FEBS Lett. 585*, 803−808.

(19) Aramini, J. M., Rossi, P., Shastry, R., Nwosu, C., Cunningham, K., Xiao, R., Liu, J., Baran, M. C., Rajan, P. K., and Acton, T. B. (2007) http://www.pdb.org/pdb/explore/explore.do?structureId=2JRF.

(20) Bradford, M. M. (1976) A rapid and sensitive method for the quantitation of microgram quantities of protein utilizing the principle of protein-dye binding. *Anal. Biochem. 72*, 248−254.

(21) Na, C. N., and Timasheff, S. N. (1986) Interaction of vinblastine with calf brain tubulin: multiple equilibria. *Biochemistry 25*, 6214−6222.

(22) Otzen, D. E., Lundvig, D. M., Wimmer, R., Nielsen, L. H., Pedersen, J. R., and Jensen, P. H. (2005) p25alpha is flexible but natively folded and binds tubulin with oligomeric stoichiometry. *Protein Sci. 14*, 1396−1409.

(23) Hlavanda, E., Klement, E., Kókai, E., Kovács, J., Vincze, O., Tőkési, N., Orosz, F., Medzihradszky, K. F., Dombrádi, V., and Ovádi, J. (2007) Phosphorylation blocks the activity of tubulin polymerization-promoting protein (TPPP): identification of sites targeted by different kinases. *J. Biol. Chem. 282*, 29531−29539.

(24) Semisotnov, G. V., Rodionova, N. A., Razgulyaev, O. I., Uversky, V. N., Gripas, A. F., and Gilmanshin, R. I. (1991) Study of the "molten globule" intermediate state in protein folding by a hydrophobic fluorescent probe. *Biopolymers 31*, 119−128.

(25) Leal, S. S., and Gomes, C. M. (2007) Studies of the molten globule state of ferredoxin: structural characterization and implications on protein folding and iron-sulfur center assembly. *Proteins 68*, 606−616.

(26) Sutovsky, H., and Gazit, E. (2004) The von Hippel-Lindau tumor suppressor protein is a molten globule under native conditions: implications for its physiological activities. *J. Biol. Chem. 279*, 17190−17196.

(27) Bodor, A., Tóth, I., Bányai, I., Szabó, Z., and Hefter, G. T. (2000) 19F NMR study of the equilibria and dynamics of the Al3+/F-system. *Inorg. Chem. 39*, 2530−2537.

(28) Bodor, A., Bányai, I., Zékány, L., and Tóth, I. (2002) Slow dynamics of aluminium-citrate complexes studied by 1H- and 13C-NMR spectroscopy. *Coord. Chem. Rev. 228*, 163−173.

(29) Berg, J. M., and Shi, Y. (1996) The galvanization of biology: a growing appreciation for the roles of zinc. *Science 271*, 1081−1085.

(30) Law, W., Kelland, E. E., Sharp, P., and Toms, N. J. (2003) Characterisation of zinc uptake into rat cultured cerebrocortical oligodendrocyte progenitor cells. *Neurosci. Lett. 352*, 113−116.

(31) Mocchegiani, E., Bertoni-Freddari, C., Marcellini, F., and Malavolta, M. (2005) Brain, aging and neurodegeneration: role of zinc ion availability. *Prog. Neurobiol. 75*, 367−390.

(32) Frederickson, C. J., Suh, S. W., Silva, D., Frederickson, C. J., and Thompson, R. B. (2000) Importance of zinc in the central nervous system: the zinc-containing neuron. *J. Nutr. 130*, 1471S−1483S.

(33) Smith, G. S., Chen, L., Bamm, V. V., Dutcher, J. R., and Harauz, G. (2010) The interaction of zinc with membrane-associated 18.5 kDa

myelin basic protein: an attenuated total reflectance-Fourier transform infrared spectroscopic study. *Amino Acids 39*, 739−750.

(34) Baran, C., Smith, G. S., Bamm, V. V., Harauz, G., and Lee, J. S. (2010) Divalent cations induce a compaction of intrinsically disordered myelin basic protein. *Biochem. Biophys. Res. Commun. 391*, 224−229.

(35) Song, Y. J., Lundvig, D. M., Huang, Y., Gai, W. P., Blumbergs, P. C., Hojrup, P., Otzen, D., Halliday, G. M., and Jensen, P. H. (2007) p25alpha relocalizes in oligodendroglia from myelin to cytoplasmic inclusions in multiple system atrophy. *Am. J. Pathol. 171*, 1291−1303.